
Benefits of Transformer: In-Context Learning in Linear Regression Tasks with Unstructured Data

Yue Xing¹ Xiaofeng Lin² Namjoon Suh² Qifan Song³ Guang Cheng²

Abstract

In practice, it is observed that transformer-based models can learn concepts in context in the inference stage. While existing literature, e.g., Zhang et al. (2023); Huang et al. (2023), provide theoretical explanations on this in-context learning ability, they assume the input x_i and the output y_i for each sample are embedded in the same token (i.e., structured data). However, in reality, they are presented in two tokens (i.e., unstructured data (Wibisono & Wang, 2023)). In this case, this paper conducts experiments in linear regression tasks to study the benefits of the architecture of transformers and provides some corresponding theoretical intuitions to explain why the transformer can learn from unstructured data. We study the exact components in a transformer that facilitate the in-context learning. In particular, we observe that (1) a transformer with two layers of softmax (self-)attentions with look-ahead attention mask can learn from the prompt if y_i is in the token next to x_i for each example; (2) positional encoding can further improve the performance; and (3) multi-head attention with a high input embedding dimension has a better prediction performance than single-head attention.

1. Introduction

With the arising of powerful large language models (LLMs) with transformer architectures, one observation is that LLM can conduct in-context learning (ICL), where the pre-trained neural network can make predictions based on contexts augmented with a small number of examples (Dong et al., 2022).

While ICL has been widely used in LLM, only limited literature is working on the theory to explain why transformers

¹Department of Statistics and Probability, Michigan State University, US. ²Department of Statistics, University of California, Los Angeles, US. ³Department of Statistics, Purdue University, US.. Correspondence to: Yue Xing <xingyue1@msu.edu>.

can learn the data in context. For example, Von Oswald et al. (2023); Ahn et al. (2023a); Akyürek et al. (2022); Zhang et al. (2023); Ahn et al. (2023b) explain how ICL learns gradient descent and linear regression models. Bai et al. (2023) studies ICL in generalized linear models, ridge regression, and LASSO. Based on Von Oswald et al. (2023); Dai et al. (2023), ICL can be connected with the gradient descent method with the provided examples in the prompt.

In recent literature, e.g., Zhang et al. (2023); Huang et al. (2023); Cheng et al. (2023), a transformer with one attention layer is proven to conduct ICL. In particular, they consider the “structured” prompt in a format of

$$E_1 = \begin{pmatrix} x_1 & x_2 & \dots & x_D & x_{\text{query}} \\ y_1 & y_2 & \dots & y_D & 0 \end{pmatrix},$$

where $\{(x_i, y_i)\}_{i \in [D]}$ is the set of in-context examples and x_{query} is the actual question of interest. Based on Zhang et al. (2023); Huang et al. (2023), the trained transformer will learn the similarity among x_{query} and x_i s and then take a weighted average over y_i s as the prediction for x_{query} .

However, there are some important missing pieces in the study of Zhang et al. (2023); Huang et al. (2023):

Separating columns of x_i and y_i In the prompt format E_1 , the same column contains both x_i and y_i . However, this is different from how the ICL is conducted in real practice – When inputting the examples, we always input the question first and then the answer. Similar to the implementation of Garg et al. (2022) and the discussion of Wibisono & Wang (2023), we want to train a transformer to conduct ICL using the following prompt format with “unstructured” data:

$$E_2 = \begin{pmatrix} x_1 & 0 & x_2 & 0 & \dots & x_D & 0 & x_{\text{query}} \\ 0 & y_1 & 0 & y_2 & \dots & 0 & y_D & 0 \end{pmatrix}.$$

In Garg et al. (2022); Wibisono & Wang (2023), it is empirically observed that deep transformers are able to learn from unstructured data. In contrast, we explicitly show the critical difference between one and two attention layers, and provide mathematical intuitions that the attention mask together with two attention layers plays an important role.

Some important components of transformers While Zhang et al. (2023); Huang et al. (2023) studies the per-

formance of a single-layer transformer, they do not further consider the following components: attention mask, positional encoding (PE), and multi-head attention.

Observing the above missing analysis, in this paper, we conduct a simulation to explore these key components that lead to the success of ICL in linear regression tasks. Our key observations are summarized in Figure 1 as follows. We believe that our observations can boost the theoretical analysis in this field.

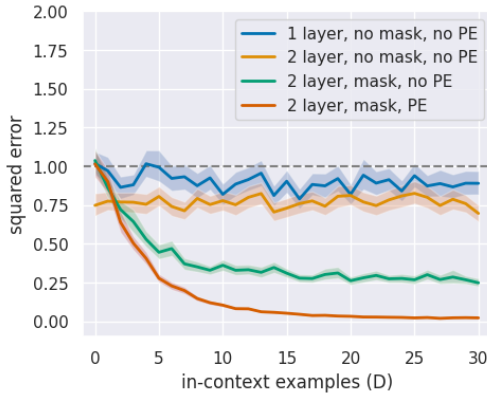


Figure 1. ICL performance with different number of layers, mask, position. Under E_2 prompt setting, we conclude that the two-layer structure and the attention mask are crucial, while positional encoding significantly improves performance.

Existing literature mainly focuses on large-scale experiments to demonstrate the effectiveness of LLMs in learning from structured/unstructured data. In contrast, in our paper, we control the experiment settings to explicitly show the benefit and interaction of each component in the transformer. In particular, our contributions are as follows:

- As in Figure 1, for the unstructured data E_2 , a one-layer transformer fails. With a two-layer transformer and a look-ahead attention mask, the transformer can conduct ICL in E_2 . Both the two-layer structure and attention mask are crucial. (Section 4)
- In Figure 1, with a two-layer transformer and attention mask, positional encoding (PE) can further improve the performance. (Section 5)
- In addition to the above key observations, multi-head attention performs better than single-head attention. With a higher input embedding dimension, the ICL performance is further improved. (Section 6)
- While both PE and large embedding dimension speed up the training process, when training with finite samples, PE improves the generalization, but large embedding dimension hurts generalization. (Section 7)

2. Related Works

Theoretical Studies The linear attention is one of the proposed methods that has been widely studied in the theoretical literature (Li et al., 2020; Katharopoulos et al., 2020; Shen et al., 2021; Zheng et al., 2022; Liu et al., 2023; Qin et al., 2022). Besides linear attention, theoretical attempts to explain the superiority of softmax attention recently emerged. In the context of ICL, several papers (SHIFTING; Gao et al., 2023; Deng et al., 2023; Chu et al., 2023; Song et al., 2023) consider ICL based on softmax regression formulation, showing that transformer attentions exhibit similar behavior with softmax regression. However, these works study the structured data format of E_1 but do not consider the unstructured data of E_2 as in our paper.

Transformer Architecture As will be introduced in the later section, there are several components in the transformer architecture considered in our paper: attention mask, multiple layers of attention, positional encoding (PE), and multi-head attention. While there are many existing studies demonstrating the success of the transformer in different areas, it is not clear the role of the components in the transformer help when learning unstructured data.

Masking is needed to prevent the attention mechanism of a transformer from “cheating” in the decoder when training (on a translating task). Other than translation tasks, attention mask has shown empirical successes in many studies, specifically in the field of computer vision and multi-modality models (Cheng et al., 2022; Fan et al., 2021; Pang et al., 2019; Harley et al., 2017; Song et al., 2020).

Another important component in transformer architecture is its compositional structure of multiple attention layers. We are aware of two works (Van Aken et al., 2019; Simoulin & Crabbé, 2021) which provided interesting analysis on the internal layer mechanisms of BERT (i.e., one of the widely used LLMs).

PE suggested by (Vaswani et al., 2017a) successfully facilitates the transformers to know the positional information of each word in the sentence. PE originally introduced for language-based models has many variants based on different data modalities; the instances include tree-based data (Shiv & Quirk, 2019), graph data (Brüel-Gabrielsson et al., 2022), time series data (Nyborg et al., 2022), video data (Ning et al., 2020), etc. Nonetheless, there is not much literature on the theoretical understanding of PE. In the context of ICL, (Bai et al., 2023) proves transformers with PE can implement more complex ICL procedures involving in-context algorithm selection.

Theoretical explorations on the advantages/properties of multi-head attention are very sparse, in sharp contrast to the rich literature on single-head attention (Li et al., 2023b;

Jelassi et al., 2022; Oymak et al., 2023; Li et al., 2023a; Huang et al., 2023). From a theoretical point of view, several works study the effects of multi-head attentions from the expressive power (Mahdavi et al., 2023), approximation (An et al., 2020), and optimization (Deora et al., 2023).

3. Notations and Architecture

In the following, we mathematically define the data distribution and the transformer architecture considered.

Data In this study, we assume all examples and the final query have an x following i.i.d. $N(0, I_d)$. The response y is a noiseless linear model, $y = x^\top \theta$, for some $\theta \sim N(0, I_d/d)$. All examples and the query share the same θ in the same prompt. For different prompts, θ s are different.

To train the transformer, we assume there are infinitely many samples of prompts with their examples and minimize the following loss

$$\mathbb{E}_{\{x_i\}_{i \in [D]}, x_{\text{query}}, \theta} \sum_{i=1}^D (y_i - \hat{y}_i)^2 + (y_{\text{query}} - \hat{y}_{\text{query}})^2.$$

where \hat{y}_i and \hat{y}_{query} are the prediction of y_i and y_{query} . As will be introduced later, for a transformer f , the output $f(E)$ has the same dimension as the input E . For the unstructured data E_2 , the output columns for $(x_i, 0)$ s are the predictions for these examples, and we take the last element in these columns as the \hat{y}_i s.

Note that for the input format E_1 , we need to query the transformer for $D + 1$ times to obtain the above loss for one task. In each query, we need to modify the matrix E_1 to obtain the corresponding \hat{y} . For example, to predict y_1 using x_1 , we only include $(x_1, 0)$ in the prompt. To predict y_2 using (x_1, y_1) and x_2 , we take $E_1 = ((x_1, y_1), (x_2, 0))$. On the other hand, when using the format of E_2 , we only need to query the transformer once: the output for the column of $(x_i, 0)$ is to predict y_i .

Single-Layer Single-Head Attention Following (Zhang et al., 2023), we start from the following simplified neural network architecture. Given an input matrix E , the output of the transformer is defined as

$$f(E) = E + W_{\text{out}} H, \quad (1)$$

where H in the single-head attention is defined as

$$H = W^V E \cdot \phi((W^K E)^\top W^Q E),$$

for some activation ϕ . The output matrix of $\phi(\cdot)$ is also known as the attention score matrix.

Attention Mask When dealing with sequential data and building an autoregressive predictive model, the (look-ahead) attention mask matrix M prevents the model from observing future tokens. Mathematically, the attention score $\phi((W^K E)^\top W^Q E)$ is modified as $\phi((W^K E)^\top W^Q E + M)$, where $M_{i,j} = 0$ if $i \leq j$, and $M_{i,j} = -\infty$ otherwise. By doing so, the attention scores of t -th token to future tokens are negligible given a column-wise softmax ϕ .

Multiple Layers of Attention To build a transformer with two attention layers, in the second layer, the input is $f(E)$, i.e., the composite of two attention layers.

Positional Encoding (PE) In GPT2, PE is designed as a matrix of weights P , to retain the information regarding the order of tokens in a prompt. Instead of feeding the original prompt matrix E to the transformer, we input $E + P$. When training the transformer, in addition to optimizing over model parameters, we also optimize over the matrix P , i.e., P is trainable.

In addition to the positional encoding in GPT2 where all elements in P are free parameters, in the literature, a sine and cosine parametric model of positional encoding P is also considered (Vaswani et al., 2017b):

$$\begin{aligned} P_{2i-1, pos} &= \sin((pos - 1)/\Lambda^{2i/d}), \\ P_{2i, pos} &= \cos((pos - 1)/\Lambda^{2i/d}), \end{aligned} \quad (2)$$

where $pos \in \{1, \dots, r\}$, $i \in \{1, \dots, d\}$, and Λ is a user-specified scalar. The value of r is $D + 1$ for E_1 and $2D + 1$ for E_2 . Figure 8 demonstrates the correlation pattern among P_i 's, i.e. the columns of P .

Input Embedding Since LLMs are designed for language data, one needs an additional step to translate discrete word tokens into numerical representations before feeding them into the LLMs. This is done by a trainable embedding matrix, which serves as a lookup table.

Following (Garg et al., 2022), we assume continuous raw input $x_i \in \mathbb{R}^d$ and embedded input $M_{in} E$ for some matrix parameter $M_{in} \in \mathbb{R}^{p \times (d+1)}$. The empirical results in this proposal train M_{in} via gradient descent. On the other hand, since M_{in} can be absorbed by other matrix parameters in the model (refer to (3)), our preliminary theoretical analysis mostly ignores the presence of M_{in} and use the raw input matrix E when using single-head attention. In multi-head attention, we study the impact of embedding dimension p .¹

¹PE is added after the input prompt passes the embedding later. As the embedding dimension is p rather than d , one needs to update the formula 2 and replace d with p .

Multi-Head Attention In the commonly used transformer structure in the literature, e.g., (Vaswani et al., 2017b), the prompt is firstly projected into an attention layer $H = \text{concat}(H_1, \dots, H_h)$, concatenating intermediate outputs H_j where H_j is the output from the j -th head (i.e., Dot-Product Attention)

$$H_j = W_j^V E \cdot \phi \left((W_j^K E)^\top W_j^Q E \right) \quad (3)$$

for some activation function ϕ , such as the linear or element-wise nonlinear activation function (Zhang et al., 2023; Vaswani et al., 2017b;b). Throughout this proposal, unless otherwise specified, ϕ is a columns-wise softmax function aiming at normalizing each column so that each column represents a probability vector, with non-negative elements with the sum of the probabilities equal to 1 in each column. For each head $j = 1, \dots, h$, parameter matrices $W_j^V, W_j^K, W_j^Q \in \mathbb{R}^{m \times p}$ with $m = p/h$. The matrix output of ϕ is called **attention score**.

Experiment Settings Throughout this paper, we modify the implementation of (Garg et al., 2022) to examine the effect of the different components in the transformer. In the tasks, we take x dimension as $d = 5$ and the number of examples in each prompt as $D = 30$. We train different models for 50k to 500k steps to ensure the convergence of optimization and the ICL prediction performance no longer changes. A bad performance under such a large number of steps implies the failure of convergence, e.g., Figure 2. Table 3 in the appendix summarizes how to control each component in the transformer. In the inference stage, to obtain an error bar (presented by the shaded area in figures), we randomly sample 1280 prompts to obtain the standard error.

4. Two-Layer Transformer + Attention Mask

In this section, we demonstrate that the two-layer structure and the attention mask together play a crucial role in ICL when the examples are in a format of E_2 .

4.1. Empirical Observation

Under E_2 , it is crucial that the transformer architecture is capable to connect each y_i with its corresponding x_i . This goal cannot be achieved without any positional information built into the model. We find that the transformer can connect x_i s to y_i s when there is more than one layer of attention, along with the attention mask.

Figure 2 demonstrates our preliminary experiment results. We take x_i dimension $d = 5$, embedding dimension $p = 64$, and number of heads $h = 8$. We use E_2 as the input to the transformer and examine the ICL performance. The left panel are transformers of one/two layers of attention, and

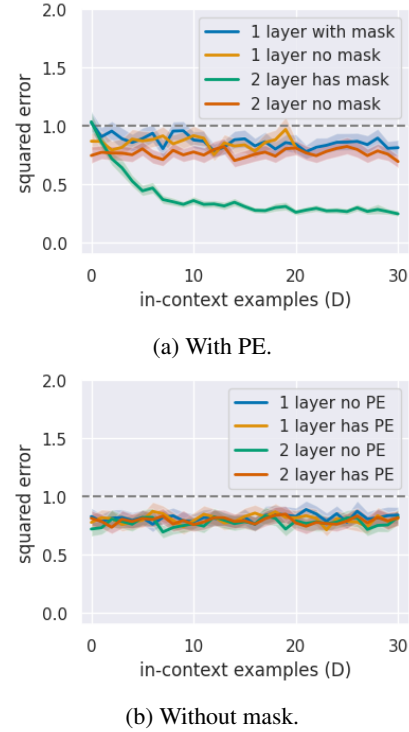


Figure 2. Performance of one-layer and two-layer transformers with/without attention mask, with/without PE (no mask).

with/without attention mask. One can see that when using a two-layer transformer together with the attention mask, the prediction loss quickly drops when increasing the number of examples D , while missing either the second layer or the attention mask results in a failure of ICL.

On the other hand, since PE encodes positional information into the system, we examine whether it helps to learn from E_2 . In the bottom plot of Figure 2, PE itself is hard to facilitate ICL from E_2 without the attention mask.

4.2. Why One-Layer Transformer Fails

In the following, we explain the poor performance of single-layer transformers. For instance, under a linear transformer (i.e., ϕ is an identity mapping) and single-head attention, when D is sufficiently large, the final output of \hat{y}_{query} approximately equals to

$$w_{\text{out}} \begin{bmatrix} \sum x_i x_i^\top + x_{\text{query}} x_{\text{query}}^\top & 0 \\ 0 & \sum y_i^2 \end{bmatrix} (W^K)^\top W^Q \begin{bmatrix} x_{\text{query}} \\ 0 \end{bmatrix},$$

where w_{out} is the last row of $W_{\text{out}} W^V$.

Consider a symmetric distribution of $\theta \sim \frac{1}{2}\delta_{\theta_0} + \frac{1}{2}\delta_{-\theta_0}$. Since both $\begin{bmatrix} \sum x_i x_i^\top + x_{\text{query}} x_{\text{query}}^\top & 0 \\ 0 & \sum y_i^2 \end{bmatrix}$ and x_{query} are almost constant regardless of the sign of θ , to minimize the loss (which takes the expectation over θ), one must have

$\hat{y}_{\text{query}} = 0$. For softmax activation ϕ , due to the symmetry of θ distribution, a similar issue happens, and the best prediction result is also 0.

In general, \hat{y}_{query} is a weighted average of the last entry across all tokens in the prompt. In a simplified scenario where $W_{p,:}^V = (0, \dots, 0, 1)$, this becomes $\hat{y}_{\text{query}} = \sum_{i=1}^D 0 \cdot \phi_{D,2i-1} + \sum_{i=1}^D y_i \cdot \phi_{D,2i}$, where $\phi_{D,k}$ is the attention score of x_{query} with the k -th token in the prompt. One attention layer, regardless of h , aims to capture the column dependency of its input prompt. Therefore, given a single layer of attention, (i) $\phi_{D,2i}$'s can only capture the dependency information between $(0, y_i)$ tokens and $(x_{\text{query}}, 0)$ and fails to deliver any useful in-context knowledge to \hat{y}_{query} ; (ii) $\phi_{D,2i-1}$'s do capture similarity information about x_i 's and x_{query} but cannot pass this information to \hat{y}_{query} as they are multiplied by 0's. This leads to the failure of \hat{y}_{query} prediction.

4.3. Why Two-Layer Transformer Succeeds

To explain why two-layer transformer + attention mask facilitates ICL in E_2 , we start from constructing a simple two-layer transformer.

In the first layer, we use a softmax attention layer with all the weights as zero in W^K and W^Q , and $W^V = I_{d+1}$. Thanks to the attention mask, this trivial first layer can perform a naive aggregation of tokens. In this case, with the attention mask, the output of the first layer is

$$f(E_2) = \begin{bmatrix} 2x_1 & \frac{1}{2}x_1 & \frac{1}{3}x_1 + \frac{4}{3}x_2 & \frac{1}{4}x_1 + \frac{1}{4}x_2 & \dots \\ 0 & \frac{3}{2}y_1 & \frac{1}{3}y_1 & \frac{1}{4}y_1 + \frac{1}{4}y_2 & \dots \end{bmatrix}. \quad (4)$$

In the second layer, taking

$$(W^K)^\top W^Q = \begin{bmatrix} I_d / \log(D) & 0 \\ 0 & 0 \end{bmatrix},$$

then we have

$$\begin{aligned} & \hat{y}_{\text{query}} \\ & \approx \frac{x_{\text{query}}^\top}{\log D} \left(\sum_i \left(\frac{1}{i} - \frac{1}{2D} \right) x_i x_i^\top \right) \theta + \frac{\epsilon}{\log D} \quad (5) \\ & \approx y_{\text{query}}, \end{aligned}$$

i.e., a linear attention in the second layer is enough to predict y_{query} . The notation ϵ represents some cross terms of $x_{\text{query}}^\top x_i x_j^\top \theta$, which is small when D is large enough. Some detailed derivations of the above formula can be found in Section A in the appendix.

On the other hand, if we remove the attention mask, then the output of the first layer becomes $E_2 + w1^\top$ for some vector w , i.e., all columns are merely added by a constant. Therefore, in the second layer, the model still cannot learn

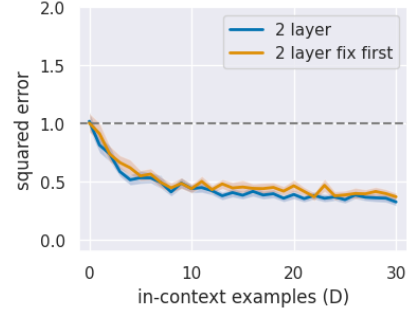


Figure 3. ICL prediction performance of training two layers together vs training the second layer only.

from the examples due to the lack of positional information.

To further justify the above analysis, we also conduct lazy training simulations. In the simulation, we fix the first layer W^Q and W^K to be zero (as in our previous analysis), and train the other parameters in the transformer. From Figure 3, there is only a slight performance difference regarding whether the first layer W^Q and W^K are fixed. It verifies the effectiveness of the lazy training regime and implies that the training of the first layer, similarly to lazy training, focuses on mixing all columns of E_2 together.

Remark 4.1. In Figure 2, in settings other than two layers + attention mask, the squared error is still slightly below 1. There are two explanations. First, the above theoretical explanation assumes there are a large number of examples D in each prompt, which is slightly different from the finite-example scenario in the experiment. Second, without an attention mask, there is some leakage of future information.

5. Positional Encoding

As mentioned in Section 3, there are some different formulations of PE: (1) completely trainable PE and (2) PE with a sin-cos parametric formulation. This section studies the effect of these different PE formulations. In short, given infinite training prompts, the completely trainable PE has a better ICL ability than the parametric formulation, and both are better than without PE.

5.1. Empirical Observation

We observe that the completely trainable PE improves the performance of the two-layer transformer for E_2 with an attention mask. Figure 4 shows the ICL performance, and Figure 7 visualizes the linear dependency of the trained P matrix in a two-layer transformer.

In Figure 4, we compare three PE methods: (i) no PE, (ii) the sin-cos formulation in (2), and (iii) the completely trainable PE. In Figure 4, the ICL performance of the transformer trained without PE is much worse than the others.

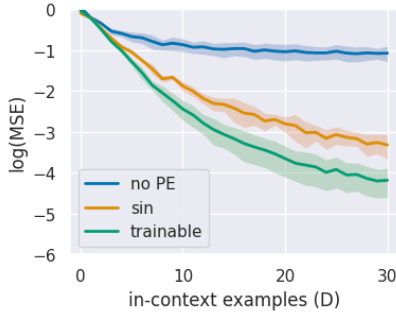


Figure 4. Comparison of different PE, ICL ability.

5.2. Why Positional Encoding Helps

To explain why PE improves the ICL performance, we draw the attention score of the two attention layers without PE (Figure 5) and with PE (Figure 6). We consider the completely trainable PE.

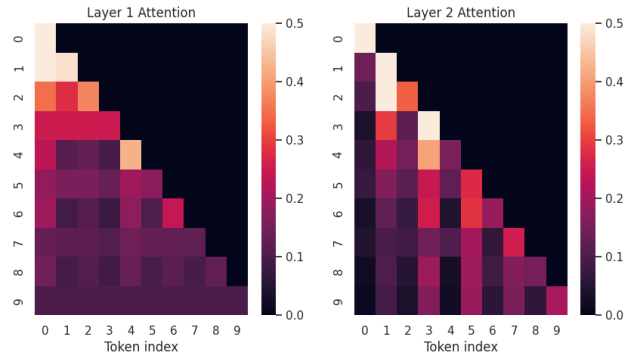


Figure 5. Attention scores of the first 5 input pairs on single head, two layer, with mask, no PE, E_2 format. One prompt. Each rows is the attention of one token.

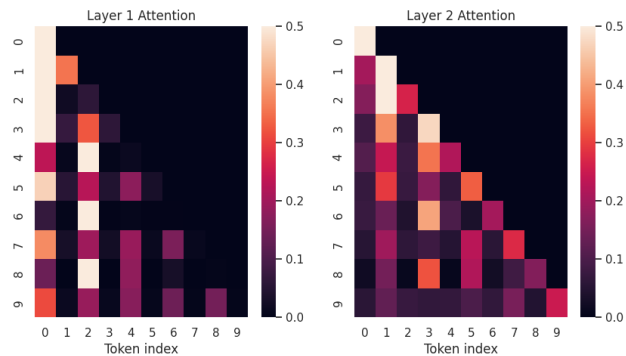


Figure 6. Attention scores of the first 5 input pairs on single head, two layer, with mask, with PE, E_2 format.

For the sake of readability of the figures, we only plot attention scores for the first 5 pairs (i.e., 10 columns) in Figure 5 and Figure 6. The full plots can be found in Figures 18 and 19 in the appendix.

There are several observations from Figure 5 and Figure 6. First, Figure 5 verifies the analysis in Section 4. In the attention score matrix of the first layer (left panel of Figure 5), the attention scores are almost the same along each row. On the other hand, in the second layer, in each row, the high scores often appear on the odd positions (position index starts from 0), which are associated with y_i s. These observations suggest that the first layer aggregates different columns, and the second layer learns from the examples and makes an ICL prediction.

Second, in the left plot in Figure 6, when adding PE, the attention scores in the first layer are almost zero for the odd positions in each row and apply a high weight for x_i s. Recall that in the formulation, the output of the first attention layer becomes

$$\begin{aligned} & f(E_2) \\ &= \underbrace{E_2}_{\text{invariant to PE}} + \underbrace{W^V E_2 \phi((W^K E_2)^\top W^Q E_2)}_{\text{change with PE}} \\ &= \begin{bmatrix} 2(x_1 + P_1^x) & w_{2,1}(x_1 + P_1^x) + (1 + w_{2,2})P_2^x & \dots \\ 2P_1^y & w_{2,1}P_1^y + (1 + w_{2,2})(y_1 + P_2^y) & \dots \end{bmatrix}, \end{aligned}$$

where $w_{i,j}$ represents the attention score of the j -th token at the i -th column. Based on Figure 6, $w_{2,1}$ gets larger and $w_{2,2}$ gets smaller. Since in $f(E_2)$, the additional E_2 outside is invariant to PE, balancing $w_{2,1}$ and $w_{2,2}$ can better align the weight for x_1 and y_1 when merging them.

For full attention map with all tokens displayed, please see 18 and 19 in appendix section D.

Third, in the left plot of Figure 6 with PE, for the rows of latter tokens, higher scores appear in later columns. This differs from the case of Figure 5 without PE. The consequence is that PE adjusts the weight of each example (x_i, y_i) in the final prediction. From equation (5) in Section 4, although all examples contribute to predicting y_{query} , the first several examples have the largest weight in the prediction, leading to a large variance. When adding PE, the weights for the latter examples get larger, controlling the variance of \hat{y}_{query} .

5.3. Comparison between Two PE Methods

While Section 5.2 explains why the completely trainable PE improves the ICL performance, in this section, we compare this PE with another parametric-formulated PE in (2).

In terms of the completely trainable PE, we examine the columns of the trained P . Figure 7 reveals that the P introduces (1) a positive correlation among x_i tokens; (2) a positive correlation among y_i tokens; and (3) a very negative correlation between x_i and y_i tokens, especially when they are far away from each other.

For PE with the parametric formulation, when changing Λ in (2), the pattern of PE also changes. In Figure 8, with a

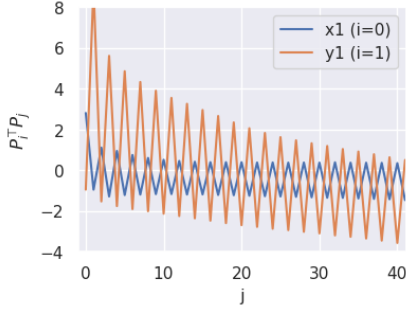


Figure 7. The value of $P_i^\top P_j$ in the completely trainable PE.

smaller Λ , $P_i^\top P_j$ tends to appear in a periodic pattern, and some neighbors will have a small attention score.

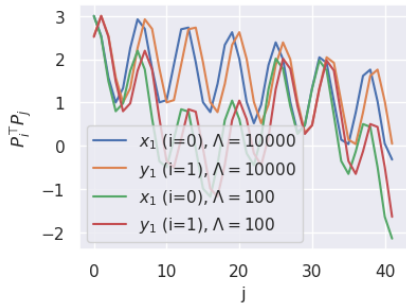


Figure 8. The value of $P_i^\top P_j$ using the formula in (2).

We also conduct experiments to compare the performance of different choices of Λ . The results are summarized in Figure 9. When taking small Λ , we observe that the ICL performance varies a lot in different trials, occasionally resulting in performances that are even worse than training with no positional encoding. As a result, we pick an average case and the worst case in Figure 17 in Appendix D.

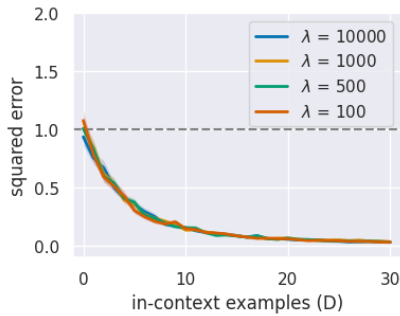


Figure 9. ICL performance when changing Λ in the sin-cos PE. The standard error is almost zero in this figure.

6. Other Benefits of the Architecture

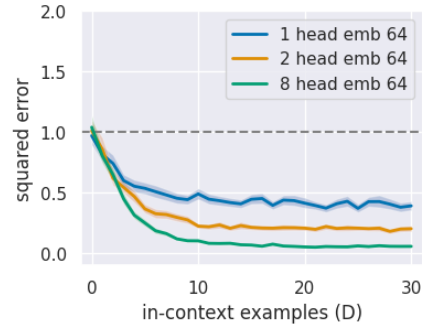
In addition to two layers of attention + attention mask and PE, there are other components in the transformer architecture. In this section, we study the effect of multi-head

attention and the input embedding dimension.

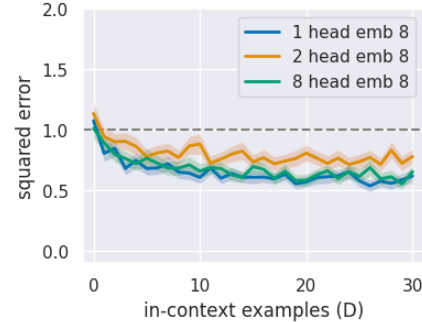
6.1. Multi-Head Attention is Preferred

In the commonly used multi-head attention structure in literature (Fang et al., 2022), the prompt is firstly projected in each head, and then the final output of the multi-head attention concatenates all the output of each head together.

We examine the ICL performance when changing the number of heads. We train two-layer transformers with attention mask, PE, input format E_2 , and with different number of heads. The results are shown in Figure 10. We use the input embedding transformation with $p = 64$ or 8. One can see that multi-head attention leads to better ICL performance when fixing the same p if p is large enough. Intuitively, when $p/h > d$, increasing h can improve the expressive power of the transformer.



(a) $p=64$



(b) $p=8$

Figure 10. ICL performance of single- and multi-head attention. With PE. Input format: E_2 .

6.2. Input Embedding Dimension

While in previous sections we observe the benefit of PE and multi-head attention, we show in this section that these two components can further benefit ICL when increasing the input embedding size p .

Since PE is added after transforming the raw input E into an embedding matrix with a large embedding dimension,

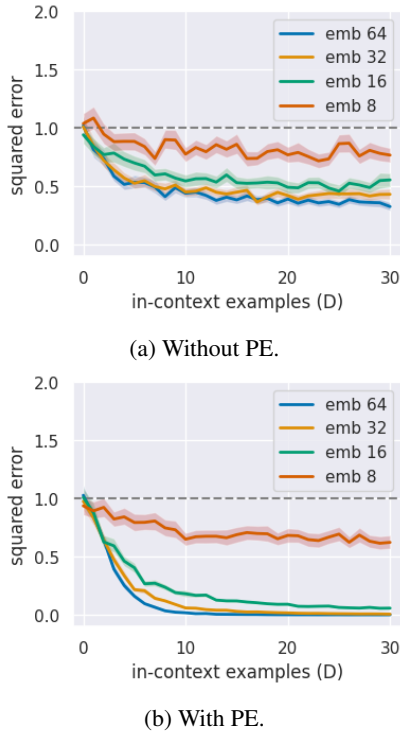


Figure 11. ICL performance when changing the number of embeddings with/without PE.

there is more flexibility in designing the matrix P . As in Figure 11, if further adding PE, the benefit of increasing the number of embeddings from 32 to 64 is greater.

In terms of multi-head attention, we also conduct experiment with a small input embedding dimension p .

7. Convergence and Generalization

While the previous section mainly focuses on the ICL performance, in this section, we study (i) the training convergence rate given an infinite number of training samples and (ii) the generalization performance assuming a fixed training size.

7.1. Training Loss

We present the training loss under different settings of PE, p , and h . In each iteration, we sample a new batch of data from data distribution to train the model and compare the ICL performance when changing the embedding dimension, number of heads, and whether PE is used.

Due to the page limit, the detailed experiment setups, results, observations, and discussions are postponed to Appendix B. In short, in the linear regression task, when adding PE into the system, the minimal training loss is smaller, and the convergence speed is much faster. When increasing the embedding dimension, one can also observe that the min-

imal training loss is smaller, and the relative convergence speed is slightly faster. In terms of the number of heads, with multiple heads, the system either converges faster or becomes more stable.

7.2. Generalization

In contrast to Section 7.1 where we sample new data in each iteration, in this section, we fix the total number of training prompts N and examine the generalization.

The experiment results and discussions are postponed to Appendix B. In short, the generalization also depends on the transformer architecture besides N and the number of training iterations. When increasing the embedding dimension p , the generalization gets worse. An interesting observation (Figure 12) is that the generalization gets significantly better with the completely trainable PE and larger N .

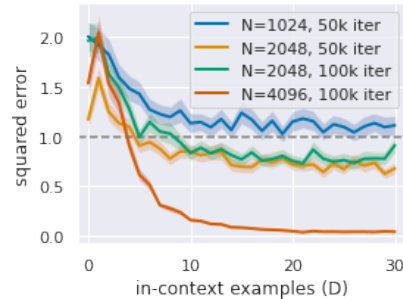


Figure 12. Training with finite samples and PE.

8. Conclusion

In this paper, we conduct experiments and explain why transformers can learn E_2 . Different from the prompt format E_1 where x and y are in the same column, E_2 separates them. When training with infinite prompts, (1) the transformer should be of at least two attention layers with the look-ahead attention mask to learn E_2 . In addition, (2) PE can further connect x and y and balance the mean and variance in the prediction loss. (3) a high embedding dimension p and multi-head attention improves the ICL performance. Finally, (4) PE generally improves the training speed and generalization, while a high embedding dimension p may lead to a worse generalization.

Our observations can potentially motivate theoretical analysis in this area. For example, (i) it is interesting to theoretically quantify the benefit from PE, large p , and multi-head attention. In addition, (ii) one may also investigate the benefit of PE when training with finite samples, as it significantly improves the generalization even with more trainable parameters. (iii) Another potential topic is to extend from the (x, y) examples to chain-of-thought.

Broader Impact

This paper studies the theoretical properties of a simple transformer architecture, and there is no new methodology introduced in this paper. As a result, there is no obvious negative social impact which must be highlighted here.

References

- Ahn, K., Cheng, X., Daneshmand, H., and Sra, S. Transformers learn to implement preconditioned gradient descent for in-context learning. *arXiv preprint arXiv:2306.00297*, 2023a.
- Ahn, K., Cheng, X., Song, M., Yun, C., Jadbabaie, A., and Sra, S. Linear attention is (maybe) all you need (to understand transformer optimization). *arXiv preprint arXiv:2310.01082*, 2023b.
- Akyürek, E., Schuurmans, D., Andreas, J., Ma, T., and Zhou, D. What learning algorithm is in-context learning? investigations with linear models. *arXiv preprint arXiv:2211.15661*, 2022.
- An, B., Lyu, J., Wang, Z., Li, C., Hu, C., Tan, F., Zhang, R., Hu, Y., and Chen, C. Repulsive attention: Rethinking multi-head attention as bayesian inference. *arXiv preprint arXiv:2009.09364*, 2020.
- Bai, Y., Chen, F., Wang, H., Xiong, C., and Mei, S. Transformers as statisticians: Provable in-context learning with in-context algorithm selection. *arXiv preprint arXiv:2306.04637*, 2023.
- Brüel-Gabrielsson, R., Yurochkin, M., and Solomon, J. Rewiring with positional encodings for graph neural networks. *arXiv preprint arXiv:2201.12674*, 2022.
- Cheng, B., Misra, I., Schwing, A. G., Kirillov, A., and Girshick, R. Masked-attention mask transformer for universal image segmentation. In *Proceedings of the IEEE/CVF conference on computer vision and pattern recognition*, pp. 1290–1299, 2022.
- Cheng, X., Chen, Y., and Sra, S. Transformers implement functional gradient descent to learn non-linear functions in context. *arXiv preprint arXiv:2312.06528*, 2023.
- Chu, T., Song, Z., and Yang, C. Fine-tune language models to approximate unbiased in-context learning. *arXiv preprint arXiv:2310.03331*, 2023.
- Dai, D., Sun, Y., Dong, L., Hao, Y., Ma, S., Sui, Z., and Wei, F. Why can gpt learn in-context? language models implicitly perform gradient descent as meta-optimizers. In *ICLR 2023 Workshop on Mathematical and Empirical Understanding of Foundation Models*, 2023.
- Deng, Y., Li, Z., Mahadevan, S., and Song, Z. Zero-th order algorithm for softmax attention optimization. *arXiv preprint arXiv:2307.08352*, 2023.
- Deora, P., Ghaderi, R., Taheri, H., and Thrampoulidis, C. On the optimization and generalization of multi-head attention. *arXiv preprint arXiv:2310.12680*, 2023.
- Dong, Q., Li, L., Dai, D., Zheng, C., Wu, Z., Chang, B., Sun, X., Xu, J., and Sui, Z. A survey for in-context learning. *arXiv preprint arXiv:2301.00234*, 2022.
- Fan, Z., Gong, Y., Liu, D., Wei, Z., Wang, S., Jiao, J., Duan, N., Zhang, R., and Huang, X. Mask attention networks: Rethinking and strengthen transformer. *arXiv preprint arXiv:2103.13597*, 2021.
- Fang, Z., Ouyang, Y., Zhou, D.-X., and Cheng, G. Attention enables zero approximation error. *arXiv preprint arXiv:2202.12166*, 2022.
- Gao, Y., Song, Z., and Xie, S. In-context learning for attention scheme: from single softmax regression to multiple softmax regression via a tensor trick. *arXiv preprint arXiv:2307.02419*, 2023.
- Garg, S., Tsipras, D., Liang, P. S., and Valiant, G. What can transformers learn in-context? a case study of simple function classes. *Advances in Neural Information Processing Systems*, 35:30583–30598, 2022.
- Harley, A. W., Derpanis, K. G., and Kokkinos, I. Segmentation-aware convolutional networks using local attention masks. In *Proceedings of the IEEE International Conference on Computer Vision*, pp. 5038–5047, 2017.
- Huang, Y., Cheng, Y., and Liang, Y. In-context convergence of transformers. *arXiv preprint arXiv:2310.05249*, 2023.
- Jelassi, S., Sander, M., and Li, Y. Vision transformers provably learn spatial structure. *Advances in Neural Information Processing Systems*, 35:37822–37836, 2022.
- Kaplan, J., McCandlish, S., Henighan, T., Brown, T. B., Chess, B., Child, R., Gray, S., Radford, A., Wu, J., and Amodei, D. Scaling laws for neural language models. *arXiv preprint arXiv:2001.08361*, 2020.
- Katharopoulos, A., Vyas, A., Pappas, N., and Fleuret, F. Transformers are rnns: Fast autoregressive transformers with linear attention. In *International conference on machine learning*, pp. 5156–5165. PMLR, 2020.
- Li, H., Wang, M., Liu, S., and Chen, P.-Y. A theoretical understanding of shallow vision transformers: Learning, generalization, and sample complexity. *arXiv preprint arXiv:2302.06015*, 2023a.

- Li, R., Su, J., Duan, C., and Zheng, S. Linear attention mechanism: An efficient attention for semantic segmentation. *arXiv preprint arXiv:2007.14902*, 2020.
- Li, Y., Ildiz, M. E., Papailiopoulos, D., and Oymak, S. Transformers as algorithms: Generalization and stability in in-context learning. 2023b.
- Liu, L., Cai, L., Zhang, C., Zhao, X., Gao, J., Wang, W., Lv, Y., Fan, W., Wang, Y., He, M., et al. Linrec: Linear attention mechanism for long-term sequential recommender systems. In *Proceedings of the 46th International ACM SIGIR Conference on Research and Development in Information Retrieval*, pp. 289–299, 2023.
- Mahdavi, S., Liao, R., and Thrampoulidis, C. Memorization capacity of multi-head attention in transformers. *arXiv preprint arXiv:2306.02010*, 2023.
- Ning, K., Xie, L., Wu, F., and Tian, Q. Polar relative positional encoding for video-language segmentation. In *IJCAI*, volume 9, pp. 10, 2020.
- Nyborg, J., Pelletier, C., and Assent, I. Generalized classification of satellite image time series with thermal positional encoding. In *Proceedings of the IEEE/CVF Conference on Computer Vision and Pattern Recognition*, pp. 1392–1402, 2022.
- Oymak, S., Rawat, A. S., Soltanolkotabi, M., and Thrampoulidis, C. On the role of attention in prompt-tuning. *arXiv preprint arXiv:2306.03435*, 2023.
- Pang, Y., Xie, J., Khan, M. H., Anwer, R. M., Khan, F. S., and Shao, L. Mask-guided attention network for occluded pedestrian detection. In *Proceedings of the IEEE/CVF international conference on computer vision*, pp. 4967–4975, 2019.
- Qin, Z., Sun, W., Deng, H., Li, D., Wei, Y., Lv, B., Yan, J., Kong, L., and Zhong, Y. cosformer: Rethinking softmax in attention. *arXiv preprint arXiv:2202.08791*, 2022.
- Shen, Z., Zhang, M., Zhao, H., Yi, S., and Li, H. Efficient attention: Attention with linear complexities. In *Proceedings of the IEEE/CVF winter conference on applications of computer vision*, pp. 3531–3539, 2021.
- SHIFTING, W. The closeness of in-context learning and weight shifting for softmax regression.
- Shiv, V. and Quirk, C. Novel positional encodings to enable tree-based transformers. *Advances in neural information processing systems*, 32, 2019.
- Simoulin, A. and Crabbé, B. How many layers and why? an analysis of the model depth in transformers. In *Proceedings of the 59th Annual Meeting of the Association for Computational Linguistics and the 11th International Joint Conference on Natural Language Processing: Student Research Workshop*, pp. 221–228, 2021.
- Song, K., Wei, X.-S., Shu, X., Song, R.-J., and Lu, J. Bimodal progressive mask attention for fine-grained recognition. *IEEE Transactions on Image Processing*, 29:7006–7018, 2020.
- Song, Z., Cai, T., Lee, J. D., and Su, W. J. Reward collapse in aligning large language models. *arXiv preprint arXiv:2305.17608*, 2023.
- Van Aken, B., Winter, B., Löser, A., and Gers, F. A. How does bert answer questions? a layer-wise analysis of transformer representations. In *Proceedings of the 28th ACM international conference on information and knowledge management*, pp. 1823–1832, 2019.
- Vaswani, A., Shazeer, N., Parmar, N., Uszkoreit, J., Jones, L., Gomez, A. N., Kaiser, L., and Polosukhin, I. Attention is all you need. *Advances in neural information processing systems*, 30, 2017a.
- Vaswani, A., Shazeer, N., Parmar, N., Uszkoreit, J., Jones, L., Gomez, A. N., Kaiser, L. u., and Polosukhin, I. Attention is all you need. In Guyon, I., Luxburg, U. V., Bengio, S., Wallach, H., Fergus, R., Vishwanathan, S., and Garnett, R. (eds.), *Advances in Neural Information Processing Systems 30*, pp. 5998–6008. Curran Associates, Inc., 2017b. URL <http://papers.nips.cc/paper/7181-attention-is-all-you-need.pdf>.
- Von Oswald, J., Niklasson, E., Randazzo, E., Sacramento, J., Mordvintsev, A., Zhmoginov, A., and Vladymyrov, M. Transformers learn in-context by gradient descent. In *International Conference on Machine Learning*, pp. 35151–35174. PMLR, 2023.
- Wibisono, K. C. and Wang, Y. On the role of unstructured training data in transformers’ in-context learning capabilities. In *NeurIPS 2023 Workshop on Mathematics of Modern Machine Learning*, 2023.
- Zhang, R., Frei, S., and Bartlett, P. L. Trained transformers learn linear models in-context. *arXiv preprint arXiv:2306.09927*, 2023.
- Zheng, L., Wang, C., and Kong, L. Linear complexity randomized self-attention mechanism. In *International Conference on Machine Learning*, pp. 27011–27041. PMLR, 2022.

Below is a summary of the appendix:

- Section A: detailed formulas for two-layer transformers.
- Section B: details for Section 7.
- Section C: details of configurations of experiments.
- Section D: additional experiment figures and tables.

A. Detailed Formulas for Two-Layer Transformer

This section provides longer formulas with derivation details for Section 4.

Below are some derivations to obtain (4) and (5).

For the lazy-training scheme, in the first layer, since $W^K = W^Q = 0$, we have

$$\phi((W^K E_2)^\top (W^Q E_2)) = \phi\left(\begin{bmatrix} 0 & 0 & \dots & 0 \\ \dots & & & \\ 0 & 0 & \dots & 0 \end{bmatrix}\right) = \begin{bmatrix} 1 & \frac{1}{2} & \frac{1}{3} & \dots & \frac{1}{2D+1} \\ 0 & \frac{1}{2} & \frac{1}{3} & \dots & \frac{1}{2D+1} \\ 0 & 0 & \frac{1}{3} & \dots & \frac{1}{2D+1} \\ \dots & & & & \\ 0 & 0 & 0 & \dots & \frac{1}{2D+1} \end{bmatrix}.$$

Further, because $W^V = I_{d+1}$, the output of the first layer becomes

$$\begin{aligned} f(E_2) &= E + E\phi((W^K E_2)^\top (W^Q E_2)) \\ &= E + \begin{bmatrix} x_1 & \frac{1}{2}x_1 & \frac{1}{3}x_1 + \frac{1}{3}x_2 & \frac{1}{4}x_1 + \frac{1}{4}x_2 & \dots & \frac{1}{2D+1}x_{\text{query}} + \frac{1}{2D+1}\sum x_i \\ 0 & \frac{1}{2}y_1 & \frac{1}{3}y_1 & \frac{1}{4}y_1 + \frac{1}{4}y_2 & \dots & \frac{1}{2D+1}\sum y_i \end{bmatrix} \\ &= \begin{bmatrix} 2x_1 & \frac{1}{2}x_1 & \frac{1}{3}x_1 + \frac{1}{3}x_2 & \frac{1}{4}x_1 + \frac{1}{4}x_2 & \dots & \frac{2D+2}{2D+1}x_{\text{query}} + \frac{1}{2D+1}\sum x_i \\ 0 & \frac{3}{2}y_1 & \frac{1}{3}y_1 & \frac{1}{4}y_1 + \frac{5}{4}y_2 & \dots & \frac{1}{2D+1}\sum y_i \end{bmatrix}, \end{aligned}$$

which is the formula (4) in Section 4.

To obtain (5), in the second layer, taking a linear ϕ and $(W^K)^\top W^Q = \begin{bmatrix} I_d/\log(D) & 0 \\ 0 & 0 \end{bmatrix}$, the last column is

$$\begin{aligned} &\phi\left(f(E_2)^\top \begin{bmatrix} I_d/\log(D) & 0 \\ 0 & 0 \end{bmatrix} f(E_2)\right)_{2D+1} \\ &= \frac{1}{\log(D)} \begin{bmatrix} 2x_1 & 0 \\ \frac{1}{2}x_1 & \frac{3}{2}y_1 \\ \frac{1}{3}x_1 + \frac{1}{3}x_2 & \frac{1}{3}y_1 \\ \frac{1}{4}x_1 + \frac{1}{4}x_2 & \frac{1}{4}y_1 + \frac{5}{4}y_2 \\ \dots & \dots \\ \frac{2D+2}{2D+1}x_{\text{query}} + \frac{1}{2D+1}\sum x_i & \frac{1}{2D+1}\sum y_i \end{bmatrix} \begin{bmatrix} \frac{2D+2}{2D+1}x_{\text{query}} + \frac{1}{2D+1}\sum x_i \\ \frac{1}{2D+1}\sum y_i \end{bmatrix} \\ &= \frac{1}{\log(D)} \begin{bmatrix} 2x_1 & 0 \\ \frac{1}{2}x_1 & \frac{3}{2}y_1 \\ \frac{1}{3}x_1 + \frac{1}{3}x_2 & \frac{1}{3}y_1 \\ \frac{1}{4}x_1 + \frac{1}{4}x_2 & \frac{1}{4}y_1 + \frac{5}{4}y_2 \\ \dots & \dots \\ \frac{2D+2}{2D+1}x_{\text{query}} + \frac{1}{2D+1}\sum x_i & \frac{1}{2D+1}\sum y_i \end{bmatrix} \left(\begin{bmatrix} \frac{2D+2}{2D+1}x_{\text{query}} \\ 0 \end{bmatrix} + \begin{bmatrix} \frac{1}{2D+1}\sum x_i \\ \frac{1}{2D+1}\sum y_i \end{bmatrix} \right), \end{aligned}$$

where

$$\frac{1}{\log(D)} \begin{bmatrix} 2x_1 & 0 \\ \frac{1}{2}x_1 & \frac{3}{2}y_1 \\ \frac{1}{3}x_1 + \frac{4}{3}x_2 & \frac{1}{3}y_1 \\ \frac{1}{4}x_1 + \frac{1}{4}x_2 & \frac{1}{4}y_1 + \frac{5}{4}y_2 \\ \dots & \dots \\ \frac{2D+2}{2D+1}x_{\text{query}} + \frac{1}{2D+1}\sum x_i & \frac{1}{2D+1}\sum y_i \end{bmatrix} \begin{bmatrix} \frac{2D+2}{2D+1}x_{\text{query}} \\ 0 \end{bmatrix} = \frac{1}{\log(D)} \frac{2D+2}{2D+1} \underbrace{\begin{bmatrix} 2x_1^\top x_{\text{query}} \\ \frac{1}{2}x_1^\top x_{\text{query}} \\ (\frac{1}{3}x_1 + \frac{4}{3}x_2)^\top x_{\text{query}} \\ \frac{1}{4}x_1^\top x_{\text{query}} + \frac{1}{4}x_2^\top x_{\text{query}} \\ \dots \\ \frac{1}{2D+2}x_{\text{query}}^\top x_{\text{query}} + \frac{1}{2D+1}(\sum x_i)^\top x_{\text{query}} \end{bmatrix}}_{:=A_1},$$

and the other term is

$$\frac{1}{\log(D)} \underbrace{\begin{bmatrix} 2x_1 & 0 \\ \frac{1}{2}x_1 & \frac{3}{2}y_1 \\ \frac{1}{3}x_1 + \frac{4}{3}x_2 & \frac{1}{3}y_1 \\ \frac{1}{4}x_1 + \frac{1}{4}x_2 & \frac{1}{4}y_1 + \frac{5}{4}y_2 \\ \dots & \dots \\ \frac{2D+2}{2D+1}x_{\text{query}} + \frac{1}{2D+1}\sum x_i & \frac{1}{2D+1}\sum y_i \end{bmatrix}}_{:=A_2} \begin{bmatrix} \frac{1}{2D+1}\sum x_i \\ \frac{1}{2D+1}\sum y_i \end{bmatrix}.$$

When last row of $W_{\text{out}}W^V$ as $[0, \dots, 0, 1]$, we have

$$\begin{aligned} & \hat{y}_{\text{query}} \\ &= f(E_2)_{d+1,:} f(E_2)^\top f(E_2)_{2D+1} / \log(D) \\ &\approx f(E_2)_{d+1,:} A_1 \\ &= \frac{1}{\log(D)} \frac{2D+2}{2D+1} \begin{bmatrix} 0 & \frac{3}{2}y_1 & \frac{1}{3}y_1 & \frac{1}{4}y_1 + \frac{5}{4}y_2 & \dots & \frac{1}{2D+1}\sum y_i \end{bmatrix} \begin{bmatrix} 2x_1^\top x_{\text{query}} \\ \frac{1}{2}x_1^\top x_{\text{query}} \\ (\frac{1}{3}x_1 + \frac{4}{3}x_2)^\top x_{\text{query}} \\ \frac{1}{4}x_1^\top x_{\text{query}} + \frac{1}{4}x_2^\top x_{\text{query}} \\ \dots \\ \frac{1}{2D+2}x_{\text{query}}^\top x_{\text{query}} + \frac{1}{2D+1}(\sum x_i)^\top x_{\text{query}} \end{bmatrix} \\ &= \frac{1}{\log(D)} \frac{2D+2}{2D+1} \left(\frac{3}{4}\theta^\top x_1 x_1^\top x_{\text{query}} + \frac{1}{9}\theta^\top x_1 x_1^\top x_{\text{query}} + \frac{1}{16}\theta^\top x_1 x_1^\top x_{\text{query}} + \frac{5}{16}\theta^\top x_1 x_1^\top x_{\text{query}} + \dots \right) + \frac{\epsilon}{\log(D)} \\ &= \frac{1}{\log(D)} x_{\text{query}}^\top \left(\sum_i \left(\frac{1}{i} - \frac{1}{2D} \right) x_i x_i^\top \right) \theta + \frac{1}{\log(D)} \epsilon \\ &\approx y_{\text{query}} \end{aligned}$$

where the term ϵ is the cross term of $y_i x_j^\top x_{\text{query}}$.

B. Additional Results in Convergence and Generalization

This section presents additional discussions in the training convergence and generalization performance for Section 7.

B.1. Training Loss

Changing Number of Embeddings We present the training loss under different settings.

In this experiment, we run 500k training iterations and sample new data in each iteration. We study the effect of changing embedding dimension p , number of heads h , and adding PE. We use completely trainable PE in this experiment. The results for changing p and PE can be found in Figure 13 for the absolute loss value (left) and a re-scaled loss value (right). In previous sections, we demonstrate that the final ICL performance in different settings is different, which implies that the final training loss is also different among settings. As a result, we re-scale the training loss so that the initial loss is 1 and the loss value in the last iteration is 0 for a fair comparison.

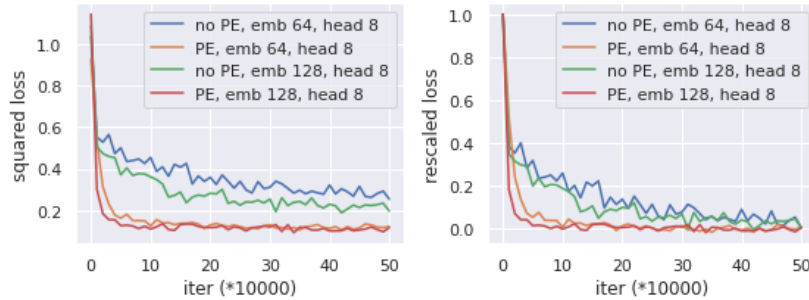


Figure 13. Training loss comparison when changing PE and embedding size p . Left: absolute loss. Right: rescaled loss.

There are some observations. First, in Figure 13, comparing the experiments with/without PE, one can see that the training becomes much faster when adding the completely trainable PE in the system. The relative training loss quickly decreases from 1 to almost 0 within 100k training steps.

Second, comparing the experiments using a higher embedding dimension, the convergence is also faster. It is intuitive that with PE, increasing to $p = 128$ makes the transformer more flexible. On the other hand, the training becomes faster via increasing p even without PE, implying a benefit of over-parametrization.

Finally, similar to (Huang et al., 2023), without PE, there are two stages of the training. At the initial stage, the training loss quickly decreases from around 1 to around 0.5 in the first 10k iterations. In the second stage, the loss slowly decreases until reaching the limit.

Changing Number of Heads Similar to the experiments of changing embedding dimension p , we change the number of heads in the transformer and examine the training speed. The results are summarized in Figure 14. One can see that the training process is more stable with more heads in the transformer when training together with PE. In addition, with PE, multi-head attention converges faster. On the other hand, without PE, the training process for single-head attention is unstable.

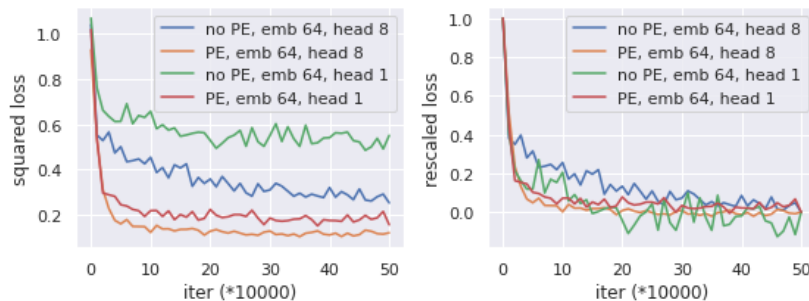


Figure 14. Training loss comparison when changing PE and embedding size p . Left: the loss value. Right: re-scaled loss.

B.2. Generalization

In contrast to Section 7.1 where we sample new data in each iteration, in this section, we fix the total number of training prompts and examine the generalization. Denote N as the number of total training prompts.

In the experiment, we change N and control PE and the embedding dimension p . We adjust the training iterations since the training loss quickly diminishes for small N . Detailed configurations are in Table 2. The results are shown in Figure 15.

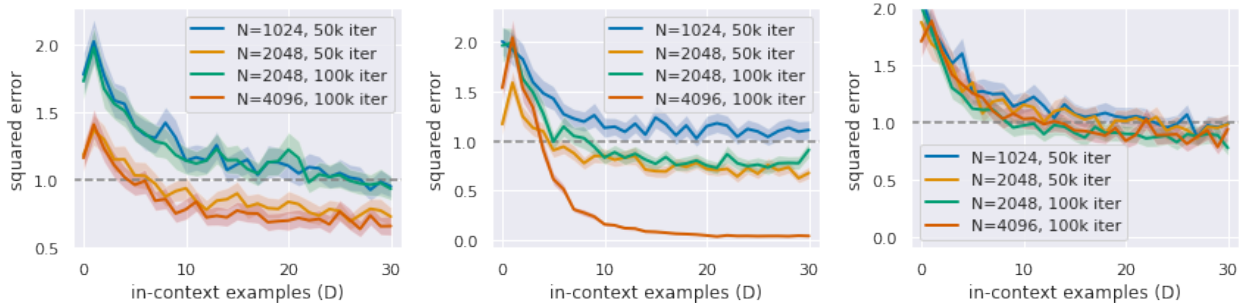


Figure 15. Training with finite samples. Left: no PE. Middle: with PE. Right: larger p .

There are several observations from Figure 15. First, when increasing N , the ICL prediction performance gets better. This is intuitive and aligns with the common understanding of the generalization.

Second, in the left plot of Figure 15, when taking $N = 2048$, the generalization is better when only trained for 50k iterations. This implies the potential benefit of early stopping.

Third, comparing the left and middle plots of Figure 15, introducing PE greatly improves the performance when $N = 4096$, and PE does not hurt the generalization when N is smaller.

Fourth, in contrast to the behavior of PE, in the right plot of Figure 15, when increasing the embedding dimension p , the generalization gets worse. To explain the different generalization performances when introducing PE and large p , we conjecture that they affect the training process in different ways, and there is no uniform theory to explain their behaviors.

Finally, in the middle plot, when taking $N = 4096$, with PE, the ICL performance for $D \in [10, 30]$ is much better than for $N = 2048$. We further plot Figure 16 below with more choices of N , and observe that the ICL performance quickly gets better when N is changing in the range of $[2000, 3000]$. To explain this, we plot the change of the loss $(\hat{y}_i - y_i)^2$ in the first 5 examples and the last 5 examples, respectively. For the first 5 examples, since $d = 5$, their loss is large and decreases slowly due to the minimax lower bound constraint. Their loss is small for the last 5 examples and decreases to almost zero. As a result, the average of all $(\hat{y}_i - y_i)^2$ s appears to be a S-shaped curve.

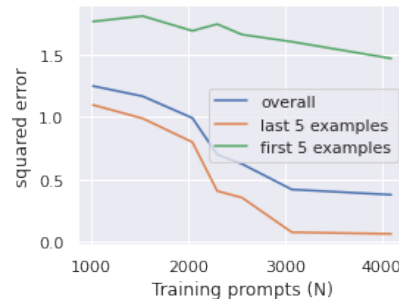


Figure 16. ICL performance when changing training size N . With trainable PE.

While the scaling law in (Kaplan et al., 2020) observed that larger LLMs are preferred when there are limited data, based on our observations in PE and input embedding dimension, we conjecture that these two components play different roles in the LLM scaling law. A rigorous theoretical justification is beyond the scope of this paper, but it is an interesting future direction.

C. Configuration Details

This section summarize the detailed configurations for the experiments in this paper.

Figure	Number of Layer	Head (h)	Embedding (p)	PE	Training Steps
Figure 2	1,2	1	64	No PE, Completely trainable PE	500k
Figure 3	2	1	64	No	500k
Figure 4	2	8	64	No PE, Completely trainable PE, sin-cos PE	500k
Figure 5	2	1	64	No	500k
Figure 6	2	1	64	Completely trainable	500k
Figure 7	2	8	64	Completely trainable	500k
Figure 8	2	8	64	sin-cos PE	500k
Figure 9	2	8	64	sin-cos PE	500k
Figure 10	2	1,2,8	8,64	Completely trainable	500k
Figure 11	2	1	8, 16, 32, 64	No PE, Completely trainable	500k
Figure 13	2	8	64, 128	Completely trainable	500k
Figure 14	2	1,8	64	Completely trainable	500k

Table 1. Settings

Plot	Training size (N)	Embedding (p)	PE	Training Steps
Left	1024	64	No	50k
Left	2048	64	No	50k
Left	2048	64	No	100k
Left	4096	64	No	100k
Middle	1024	64	Completely trainable	50k
Middle	2048	64	Completely trainable	50k
Middle	2048	64	Completely trainable	100k
Middle	4096	64	Completely trainable	100k
Right	1024	128	No	50k
Right	2048	128	No	50k
Right	2048	128	No	100k
Right	4096	128	No	100k

Table 2. Settings for Figure 15, two layers of attention with 8 heads.

Purpose	Change
Change number of layers.	Change GPT2 configuration.
Change input embedding dimension.	Change the configuration in (Garg et al., 2022).
Change PE.	Change <code>wpe</code> in the GPT2 model.
Remove attention mask.	Set all elements to 1 in <code>bias</code> in the attention layer.
Set W^K and W^Q as zero.	Force the first 2/3 rows of <code>c_attn.weights</code> and intercept terms in the attention as zero.

Table 3. Instruction in controlling the components in the transformer.

D. Other Additional Experiment Results

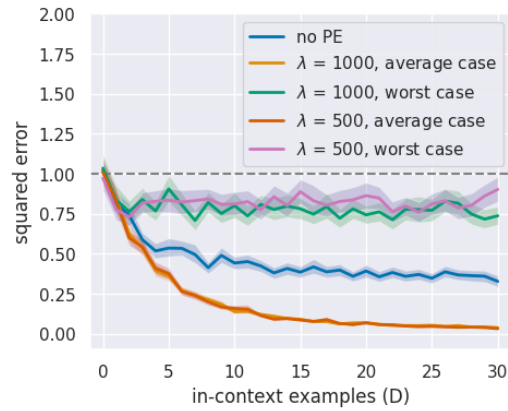


Figure 17. The average and worst cases in sin-cos PE under different λ values. Small λ values occasionally generates losses that are event greater than training without PE.

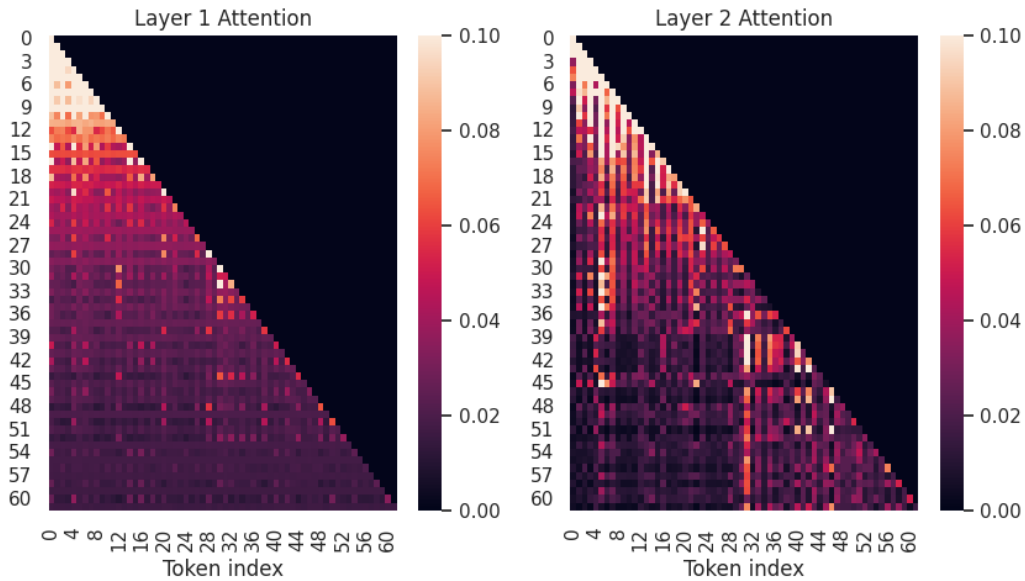


Figure 18. Full attention scores on single head, two layer, with mask, no PE, E_2 format. There are $30+1$ pairs of x and y , thus $31 * 2 = 62$ tokens in the prompt. Only attentions score from one example is shown. Each rows is the attention of one token.

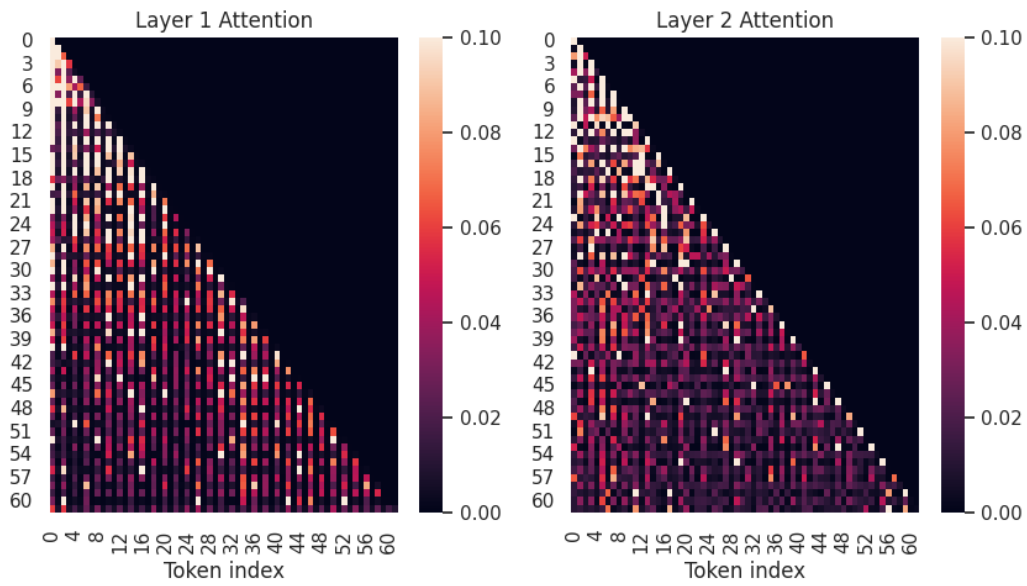


Figure 19. Full attention scores on single head, two layer, with mask, with PE, E_2 format.